

Navigation Systems Based on Multiple Bearing Measurements

PEDRO BATISTA, Member, IEEE
CARLOS SILVESTRE, Member, IEEE
PAULO OLIVEIRA, Senior Member, IEEE
Institute for Systems and Robotics
Lisbon, Portugal

This paper presents two navigation filters based on multiple bearing measurements. In the first, the state is augmented and an equivalent linear system is derived, while in the second the output of the system is modified in such a way that the resulting system is linear. In both cases, the design of a filtering solution relies on linear systems theory, in spite of the nonlinear nature of the system, and the resulting error dynamics can be made globally exponentially stable by applying, for example, Kalman filters. The continuous/discrete nature of the different measurement sources is taken into account, with the updates occurring in discrete time, while open-loop propagation is carried out between bearing measurements. Simulation results are presented, including Monte Carlo runs and a comparison with both the extended Kalman filter and the Bayesian Cramér–Rao bound, to assess the performance of the proposed solutions.

Manuscript received July 10, 2014; revised February 16, 2015; released for publication May 3, 2015.

DOI. No. 10.1109/TAES.2015.140515.

Refereeing of this contribution was handled by A. Dempster.

This work was partially supported by the Fundação para a Ciência e a Tecnologia (FCT) through Institute for Systems and Robotics (ISR), under Laboratory for Robotics and Engineering Systems (LARSyS) (UID/EEA/50009/2013) and through Institute for Mechanical Engineering (IDMEC), under Associated Laboratory for Energy, Transports and Aeronautics (LAETA) (UID/EMS/50022/2013) projects, and by the Macau Science & Technology Development Fund (FDCT) through Grant FDCT/065/2014/A, as well as by project MYRG2015-00127-FST of the University of Macau.

Authors' addresses: P. Batista, C. Silvestre, P. Oliveira, Institute for Systems and Robotics, Laboratory of Robotics and Engineering Systems, Av. Rovisco Pais, 1, 1049-001 Lisboa, Portugal. P. Batista is also with the Instituto Superior Técnico, Universidade de Lisboa, Av. Rovisco Pais, 1, 1049-001 Lisboa, Portugal. E-mail: (pbatista@isr.ist.utl.pt); C. Silvestre is with the Department of Electrical and Computer Engineering of the Faculty of Science and Technology of the University of Macau, E11 Avenida da Universidade, Taipa, Macau, China, on leave from Instituto Superior Técnico, Universidade de Lisboa, Av. Rovisco Pais, 1, 1049-001, Lisboa, Portugal; P. Oliveira is also with LAETA and the Department of Mechanical Engineering, Instituto Superior Técnico, Universidade de Lisboa, Av. Rovisco Pais, 1, 1049-001 Lisboa, Portugal.

0018-9251/15/\$26.00 © 2015 IEEE

I. INTRODUCTION

A common problem in the development of autonomous vehicles, as well as sophisticated human-operated vehicles, is that of designing the navigation system. While many different solutions exist, (pseudo)distance measurements, particularly to more than one landmark, are one of the most popular choices and are very effective in long-baseline (LBL) configurations. This paper considers bearing measurements to multiple landmarks as an alternative to distance measurements in the design of navigation systems, and two different solutions are proposed.

The celebrated GPS system is usually the workhorse of the navigation systems designed for open-space operation (e.g., [1] and references therein). In underwater applications LBL acoustic positioning systems are often employed, as electromagnetic waves suffer from significant attenuation in this medium, preventing the use of GPS. In [2], three acoustic transponders with known inertial positions are considered and an extended Kalman filter (EKF) coupled with a smoothing algorithm is proposed to estimate the system state. In [3], a typical LBL positioning system is combined with a Doppler sonar, as well as a magnetometer and roll/pitch sensors, and complementary filtering concepts are applied to show that the LBL rate and Doppler precision can be improved. In [4], two different strategies are presented. In the so-called fix computation approach, dead reckoning is performed between acoustic fixes, which reset the vehicle position whenever available. In the second, so-called filtering approach, dead reckoning is performed but, whenever available, travel times are used to correct drift resulting from the dead reckoning. Preliminary fields trials are reported in [5], where a navigation system is used that employs an LBL acoustic positioning system, a Doppler sonar, a fiber-optic north-seeking gyro, pressure sensors, and magnetic compasses. A different concept, where the aim is to estimate a segment of the trajectory instead of the current position, is proposed in [6], where diffusion-based trajectory observers are considered.

The use of single range measurements as a cheaper alternative to LBL navigation has been considered in several recent contributions, leveraging results for target localization based on range measurements. In [7] a recursive least-squares fading-memory filtering solution is proposed, and the dependence of the covariance of the estimated target on the velocity profile of the vehicle is discussed. An EKF is proposed in [8] as a solution to the problem of navigation based on range measurements to a single source, while an algebraic approach to the same problem can be found in [9]. A complete integrated navigation system, aided by range measurements, is simulated in [10], where a multirate EKF provides the filtering solution. The duality between navigation and source localization based on single range measurements is evidenced in [11], where a novel solution is also proposed with globally exponentially stable error dynamics.

An alternative to single range measurements is the use of bearing measurements; see, for example, [12], where the estimation error dynamics are shown to be globally exponentially stable under an appropriate persistent excitation condition and a circumnavigation control law is also proposed. Earlier work on the observability issues of target motion analysis based on angle readings in 2-D can be found in [13], which was later extended to 3-D in [14]. The specific observability criteria thereby derived resort to complicated nonlinear differential equations, and some tedious mathematics are needed for the solution, giving conditions that are necessary for system observability. The problem of localization of a mobile robot using bearing measurements is also addressed in [15], where a nonlinear transformation of the measurement equation into a higher dimensional space is performed. This has allowed for tight, possibly complex-shaped bounding sets for the feasible states in a closed-form representation. The problem of bearings-only target motion analysis is considered in [16], where its observability is discussed in a discrete-time setup and some insights into the optimization of observer maneuvers are provided. The posterior Cramér–Rao bounds are discussed in [17] and a hierarchical particle filter proposed in [18]. An alternative solution, based on the cubature Kalman filter, is presented in [19].

In previous work [20], we have addressed the problems of source localization and navigation based on bearing measurements to a single source in a continuous-time framework, where the duality between both problems is again evidenced. In practice, the bearing measurements are often acquired in discrete time, which poses challenges in terms of both observability analysis and filter design, leading to the extension presented in [21], where discrete-time bearing measurements to a single source are considered.

This paper addresses the problem of navigation based on multiple bearing measurements. More specifically, the vehicle is assumed to be equipped with a relative velocity sensor, an attitude and heading reference system (AHRS), and bearing sensors. This paper aims to estimate its inertial position and velocity. To solve the problem, two different solutions are proposed: In the first solution, state augmentation is performed, including the range in the system state, and an artificial output is derived such that the system as a whole is linear in the state; and in the second solution, the original nonlinear output is rewritten in such a way that the system is linear in the state, even though no state augmentation is performed. Common to both solutions is a constructive observability analysis, using linear systems theory, which enables the design of Kalman filters with globally exponentially stable error dynamics. The multirate characteristics of the sensors are also accounted for in both filter designs.

The paper is organized as follows. In Section II, the problem considered in the paper and the nominal system dynamics are introduced. The first solution is derived and analyzed in Section III, whereas the second solution is presented in Section IV. Simulation results, including

Monte Carlo runs and comparison with both the EKF and the Bayesian Cramér–Rao bound, are discussed in Section V. Finally, Section VI summarizes the main results of the paper.

A. Notation

Throughout the paper, the symbols $\mathbf{0}$ and \mathbf{I} denote a matrix of 0s and the identity matrix, respectively, while $\text{diag}(\mathbf{A}_1, \dots, \mathbf{A}_n)$ is a block diagonal matrix. The special orthogonal group is denoted by $SO(3) := \{\mathbf{X} \in \mathbb{R}^{3 \times 3} : \mathbf{X}^T \mathbf{X} = \mathbf{I}, \det(\mathbf{X}) = 1\}$, and the set of unit vectors is defined as $S(2) := \{\mathbf{x} \in \mathbb{R}^3 : \|\mathbf{x}\| = 1\}$.

II. PROBLEM STATEMENT

Consider a vehicle moving in a mission scenario where a set of landmarks are fixed, and suppose that the vehicle measures the bearing to each of the landmarks. The vehicle is assumed to be moving relatively to a fluid, which has constant velocity. Further consider that the vehicle is equipped with a relative velocity sensor and an AHRS that provides its attitude. The problem considered in this paper is that of designing an estimator for the position and velocity of the vehicle based on the available data.

Denote by $\{I\}$ an inertial coordinate reference frame and by $\{B\}$ a coordinate frame attached to the vehicle, usually called the body-fixed frame. Let $\mathbf{p}(t) \in \mathbb{R}^3$ be the inertial position of the vehicle, and denote by $\mathbf{v}(t) \in \mathbb{R}^3$ its inertial velocity, expressed in $\{I\}$, such that $\dot{\mathbf{p}}(t) = \mathbf{v}(t)$. Let the inertial velocity of the fluid be $\mathbf{v}_f(t) \in \mathbb{R}^3$, expressed in inertial coordinates, and denote by $\mathbf{v}_r(t) \in \mathbb{R}^3$ the velocity of the vehicle relative to the fluid, expressed in $\{B\}$, as measured by the relative velocity sensor. Therefore,

$$\mathbf{v}(t) = \mathbf{R}(t) \mathbf{v}_r(t) + \mathbf{v}_f(t),$$

where $\mathbf{R}(t) \in SO(3)$ is the rotation matrix from $\{B\}$ to $\{I\}$, which is provided by the AHRS. Finally, let $\mathbf{s}_i \in \mathbb{R}^3$, $i = 1, \dots, L$, denote the inertial positions of the landmarks. Then the bearing measurements are given by

$$\mathbf{d}_i(k) = \mathbf{R}^T(t_k) \frac{\mathbf{s}_i - \mathbf{p}(t_k)}{\|\mathbf{s}_i - \mathbf{p}(t_k)\|} \in S(2), \quad (1)$$

$i = 1, \dots, L$, with $t_k = t_0 + kT$, $k \in \mathbb{N}$, where $T > 0$ is the sampling period and t_0 is the initial time.

Assuming that the velocity of the fluid $\mathbf{v}_f(t)$ is constant, the nominal system dynamics can be written as

$$\begin{cases} \dot{\mathbf{p}}(t) = \mathbf{v}_f(t) + \mathbf{R}(t) \mathbf{v}_r(t) \\ \dot{\mathbf{v}}_r(t) = \mathbf{0} \\ \mathbf{d}_1(k) = \mathbf{R}^T(t_k) \frac{\mathbf{s}_1 - \mathbf{p}(t_k)}{\|\mathbf{s}_1 - \mathbf{p}(t_k)\|} \\ \vdots \\ \mathbf{d}_L(k) = \mathbf{R}^T(t_k) \frac{\mathbf{s}_L - \mathbf{p}(t_k)}{\|\mathbf{s}_L - \mathbf{p}(t_k)\|} \end{cases} \quad (2)$$

The problem considered here is that of designing an estimator for the nonlinear continuous/discrete system (2), given $\mathbf{v}_r(t)$, $\mathbf{R}(t)$, and $\mathbf{d}_i(t_k)$, $i = 1, \dots, L$, with globally exponentially stable error dynamics.

A. Discrete-Time System Dynamics

As the bearing measurements, which are used to drive the estimation error to zero, are only available at discrete-time instants, it is of interest to compute the equivalent discrete-time system dynamics, which are given by

$$\begin{cases} \mathbf{p}(t_{k+1}) = \mathbf{p}(t_k) + T\mathbf{v}_f(t_k) + \mathbf{u}(k) \\ \mathbf{v}_f(t_{k+1}) = \mathbf{v}_f(t_k) \\ \mathbf{d}_1(k) = \mathbf{R}^T(t_k) \frac{\mathbf{s}_1 - \mathbf{p}(t_k)}{\|\mathbf{s}_1 - \mathbf{p}(t_k)\|} \\ \vdots \\ \mathbf{d}_L(k) = \mathbf{R}^T(t_k) \frac{\mathbf{s}_L - \mathbf{p}(t_k)}{\|\mathbf{s}_L - \mathbf{p}(t_k)\|} \end{cases}, \quad (3)$$

with

$$\mathbf{u}(k) := \int_{t_k}^{t_{k+1}} \mathbf{R}(\tau) \mathbf{v}_f(\tau) d\tau.$$

In practice, one aims at determining an estimator for the discrete-time nonlinear system (3), as the measurements that are used to drive the estimation error to zero are available in discrete time. As the other measurements are available in continuous time (or at high rates), open-loop propagation of the state estimates can be carried out between bearing updates to yield estimates in continuous time (or at high rates). This will be detailed later.

III. FILTER DESIGN WITH STATE AUGMENTATION

A. State Augmentation

This section details a state augmentation procedure that allows us to obtain a linear system useful for the design of an estimator for the nonlinear system (3). In short, the distances to each landmark are added to the system state, their dynamics are derived as a function of the whole state, and the output is redefined considering the added states so that the system can be regarded as linear.

Define as system states

$$\begin{cases} \mathbf{x}_1(k) := \mathbf{p}(t_k) \\ \mathbf{x}_2(k) := \mathbf{v}_f(t_k) \\ x_3(k) := \|\mathbf{s}_1(k) - \mathbf{p}(t_k)\| \\ \vdots \\ x_{2+L}(k) := \|\mathbf{s}_L(k) - \mathbf{p}(t_k)\| \end{cases}, \quad (4)$$

where the distances between each landmark and the vehicle are included as additional states. In order to derive the dynamics of the additional states, notice that from (1) it is possible to write

$$x_{2+i}(k+1) \mathbf{d}_i(k+1) = \mathbf{R}^T(t_{k+1}) [\mathbf{s}_i - \mathbf{x}_1(k+1)], \quad (4)$$

$i = 1, \dots, L$. Now, left-multiplying both sides of (4) by $\mathbf{d}_i^T(k+1)$ and using the dynamics for $\mathbf{x}_1(k)$ given by (3)

yields

$$\begin{aligned} x_{2+i}(k+1) &= \mathbf{d}_i^T(k+1) \mathbf{R}^T(t_{k+1}) \mathbf{s}_i \\ &\quad - \mathbf{d}_i^T(k+1) \mathbf{R}^T(t_{k+1}) \mathbf{x}_1(k) \\ &\quad - T \mathbf{d}_i^T(k+1) \mathbf{R}^T(t_{k+1}) \mathbf{x}_2(k) \\ &\quad - \mathbf{d}_i^T(k+1) \mathbf{R}^T(t_{k+1}) \mathbf{u}(k), \end{aligned} \quad (5)$$

$i = 1, \dots, L$. The evolution of $x_{2+i}(k)$ described by (5) is undesirable, as $x_{2+i}(k+1)$ does not depend on $x_{2+i}(k)$. In order to avoid that, take (4) at time t_k , which gives

$$x_{2+i}(k) \mathbf{d}_i(k) = \mathbf{R}^T(t_k) [\mathbf{s}_i - \mathbf{x}_1(k)], \quad (6)$$

$i = 1, \dots, L$. Left-multiplying both sides of (6) by $\mathbf{R}(t_k)$ gives

$$\mathbf{s}_i - \mathbf{x}_1(k) = x_{2+i}(k) \mathbf{R}(t_k) \mathbf{d}_i(k),$$

which allows us to rewrite (5) as

$$\begin{aligned} x_{2+i}(k+1) &= -T \mathbf{d}_i^T(k+1) \mathbf{R}^T(t_{k+1}) \mathbf{x}_2(k) \\ &\quad + \mathbf{d}_i^T(k+1) \mathbf{R}^T(t_{k+1}) \mathbf{R}(t_k) \mathbf{d}_i(k) x_{2+i}(k) \\ &\quad - \mathbf{d}_i^T(k+1) \mathbf{R}^T(t_{k+1}) \mathbf{u}(k), \end{aligned} \quad (7)$$

$i = 1, \dots, L$. Finally, left-multiply both sides of (4) by $\mathbf{R}(t_{k+1})$, which allows us to write

$$\mathbf{x}_1(k+1) + x_{2+i}(k+1) \mathbf{R}(t_{k+1}) \mathbf{d}_i(k+1) = \mathbf{s}_i, \quad (8)$$

$i = 1, \dots, L$.

Define the augmented state vector

$$\mathbf{x}(k) := \begin{bmatrix} \mathbf{x}_1(k) \\ \mathbf{x}_2(k) \\ x_3(k) \\ \vdots \\ x_{2+L}(k) \end{bmatrix} \in \mathbb{R}^{3+3+L}.$$

Discarding the original nonlinear output (1) and considering (8) instead allows us to write the discrete-time linear system

$$\begin{cases} \mathbf{x}(k+1) = \mathcal{A}(k) \mathbf{x}(k) + \mathcal{B}(k) \mathbf{u}(k) \\ \mathbf{y}(k+1) = \mathcal{C}(k+1) \mathbf{x}(k+1) \end{cases}, \quad (9)$$

where

$$\mathcal{A}(k) := \begin{bmatrix} \mathbf{I} & T\mathbf{I} & \mathbf{0} \\ \mathbf{0} & \mathbf{I} & \mathbf{0} \\ \mathbf{0} & -T \mathbf{d}_1^T(k+1) \mathbf{R}^T(t_{k+1}) & \\ \vdots & \vdots & \mathcal{A}_{33}(k) \\ \mathbf{0} & -T \mathbf{d}_L^T(k+1) \mathbf{R}^T(t_{k+1}) & \end{bmatrix}$$

$$\in \mathbb{R}^{(3+3+L) \times (3+3+L)},$$

$$\mathcal{A}_{33}(k) := \text{diag}(\mathbf{d}_1^T(k+1) \mathbf{R}^T(t_{k+1}) \mathbf{R}(t_k) \mathbf{d}_1(k), \dots,$$

$$\mathbf{d}_L^T(k+1) \mathbf{R}^T(t_{k+1}) \mathbf{R}(t_k) \mathbf{d}_L(k)),$$

$$\mathcal{B}(k) := \begin{bmatrix} \mathbf{I} \\ \mathbf{0} \\ -\mathbf{d}_1^T(k+1)\mathbf{R}^T(t_{k+1}) \\ \vdots \\ -\mathbf{d}_L^T(k+1)\mathbf{R}^T(t_{k+1}) \end{bmatrix} \in \mathbb{R}^{(3+3+L) \times 3},$$

and

$$\mathcal{C}(k) := \begin{bmatrix} \mathbf{I} & \mathbf{0} & \mathbf{R}(t_k)\mathbf{d}_1(k) & \mathbf{0} & \mathbf{0} \\ \vdots & \vdots & & \ddots & \\ \mathbf{I} & \mathbf{0} & \mathbf{0} & \mathbf{0} & \mathbf{R}(t_k)\mathbf{d}_L(k) \end{bmatrix} \in \mathbb{R}^{3L \times (3+3+L)}.$$

B. Observability Analysis of the Augmented System

The observability of the linear discrete-time system (9) is detailed in the following theorem.

THEOREM 1 Suppose that, for some time $k_a \geq k_0$, there exist $i, j, l, m \in \{1, \dots, L\}$ such that

$$\mathbf{d}_i(k_a) \neq \alpha_1 \mathbf{d}_j(k_a) \quad (10)$$

and

$$\mathbf{d}_l(k_a + 1) \neq \alpha_2 \mathbf{d}_m(k_a + 1) \quad (11)$$

for all $\alpha_1, \alpha_2 \in \mathbb{R}$. Then the discrete-time linear system (9) is observable on $[k_a, k_a + 2]$ —i.e., the initial state $\mathbf{x}(k_a)$ is uniquely determined by the input $\{\mathbf{u}(k): k = k_a, k_a + 1\}$ and the output $\{\mathbf{y}(k): k = k_a, k_a + 1\}$.

PROOF The proof reduces to showing that the observability matrix $\mathcal{O}(k_a, k_a + 2)$ associated with the pair $(\mathcal{A}(k), \mathcal{C}(k))$ on $[k_a, k_a + 2]$, $k_a \geq k_0$, has rank equal to the number of states of the system. Fix $k_a \geq k_0$ and suppose that the rank of the observability matrix is less than the number of states of the system. Then there exists a unit vector

$$\mathbf{c} = \begin{bmatrix} \mathbf{c}_1^T \\ \mathbf{c}_2^T \\ c_3 \\ \vdots \\ c_{2+L} \end{bmatrix} \in \mathbb{R}^{3+3+L},$$

with $\mathbf{c}_1, \mathbf{c}_2 \in \mathbb{R}^3$, $c_3, \dots, c_{2+L} \in \mathbb{R}$, such that $\mathcal{O}(k_a, k_a + 2)\mathbf{c} = \mathbf{0}$ or, equivalently,

$$\begin{cases} \mathcal{C}(k_a)\mathbf{c} = \mathbf{0} \\ \mathcal{C}(k_a + 1)\mathbf{A}(k_a)\mathbf{c} = \mathbf{0} \end{cases} \quad (12)$$

Expanding the first equation of (12) gives

$$\begin{cases} \mathbf{c}_1 + c_3 \mathbf{R}(t_{k_a}) \mathbf{d}_1(k_a) = \mathbf{0} \\ \vdots \\ \mathbf{c}_1 + c_{2+L} \mathbf{R}(t_{k_a}) \mathbf{d}_L(k_a) = \mathbf{0} \end{cases} \quad (13)$$

Under the conditions of the theorem, there exist $i, j \in \{1, \dots, L\}$ such that (10) holds for all α_1 . Taking the difference between the i th and j th equations of (13) gives

$$c_{2+i} \mathbf{R}(t_{k_a}) \mathbf{d}_i(k_a) - c_{2+j} \mathbf{R}(t_{k_a}) \mathbf{d}_j(k_a) = \mathbf{0}$$

or, equivalently,

$$c_{2+i} \mathbf{d}_i(k_{i_a}) - c_{2+j} \mathbf{d}_j(k_{i_a}) = \mathbf{0}. \quad (14)$$

If (10) holds for all α_1 , then the only solution of (14) is

$$c_{2+i} = c_{2+j} = 0. \quad (15)$$

In turn, substituting (15) in the i th or j th equation of (13) allows us to conclude that

$$\mathbf{c}_1 = \mathbf{0}. \quad (16)$$

Substituting (16) in the remaining equations of (13) gives

$$c_{2+1} = c_{2+2} = \dots = c_{2+L} = 0. \quad (17)$$

Now, substituting (16) and (17) in the second equation of (12) allows us to write

$$\begin{cases} T[\mathbf{I} - \mathbf{R}(t_{k_a+1})\mathbf{d}_1(k_a + 1)\mathbf{d}_1^T(k_a + 1)\mathbf{R}^T(t_{k_a+1})]\mathbf{c}_2 = \mathbf{0} \\ \vdots \\ T[\mathbf{I} - \mathbf{R}(t_{k_a+1})\mathbf{d}_L(k_a + 1)\mathbf{d}_L^T(k_a + 1)\mathbf{R}^T(t_{k_a+1})]\mathbf{c}_2 = \mathbf{0} \end{cases}$$

or, equivalently,

$$\begin{cases} [\mathbf{I} - \mathbf{d}_1(k_a + 1)\mathbf{d}_1^T(k_a + 1)]\mathbf{R}^T(t_{k_a+1})\mathbf{c}_2 = \mathbf{0} \\ \vdots \\ [\mathbf{I} - \mathbf{d}_L(k_a + 1)\mathbf{d}_L^T(k_a + 1)]\mathbf{R}^T(t_{k_a+1})\mathbf{c}_2 = \mathbf{0} \end{cases} \quad (18)$$

Under the conditions of the theorem, (11) holds for all α_2 , which in turn implies that the only solution of (18) is $\mathbf{c}_2 = \mathbf{0}$. But this contradicts the hypothesis of the existence of a unit vector \mathbf{c} such that $\mathcal{O}(k_a, k_a + 2)\mathbf{c} = \mathbf{0}$, which means that the observability matrix $\mathcal{O}(k_a, k_a + 2)$ must have rank equal to the number of states of the system—and thus the system is observable, which concludes the proof.

C. Observability of the Nonlinear System

In Section III-A a state augmentation procedure was presented that leads to a linear time-varying system related to the original nonlinear system. Its observability was characterized in Section III-B, and in this section its usefulness for the design of an estimation solution for the original nonlinear system is demonstrated. Sufficient conditions for the observability of the nonlinear system (3) are derived in the following theorem, which also relates the augmented system (9) with the nonlinear system (3).

THEOREM 2 Suppose that the conditions of Theorem 1 hold for some $k_a \geq k_0$. Then:

- 1) The nonlinear system (3) is observable on the interval $[k_a, k_a + 2]$ in the sense that the initial state $\{\mathbf{p}(t_{k_a}), \mathbf{v}_f(t_{k_a})\}$ is uniquely determined by the input $\{\mathbf{u}(k): k = k_a, k_a + 1\}$ and the output $\{\mathbf{d}_1(k), \dots, \mathbf{d}_L(k): k = k_a, k_a + 1\}$; and

2) the initial condition of the augmented system (9) matches that of (3), i.e.,

$$\begin{cases} \mathbf{x}_1(k_a) = \mathbf{p}(t_{k_a}) \\ \mathbf{x}_2(k_a) = \mathbf{v}_f(t_{k_a}) \\ x_3(k_a) = \|\mathbf{s}_1 - \mathbf{p}(t_{k_a})\| \\ \vdots \\ x_{2+L}(k_a) = \|\mathbf{s}_L - \mathbf{p}(t_{k_a})\| \end{cases} .$$

PROOF Let

$$\mathbf{x}(k_a) := \begin{bmatrix} \mathbf{x}_1(k_a) \\ \mathbf{x}_2(k_a) \\ x_3(k_a) \\ \vdots \\ x_{2+L}(k_a) \end{bmatrix} \in \mathbb{R}^{3+3+L}$$

be the initial condition of (9) and let $\mathbf{p}(t_{k_a})$ and $\mathbf{v}_f(t_{k_a})$ be the initial condition of (3). From the output of (9) for $k = k_a$, it must be true that

$$\begin{cases} \mathbf{x}_1(k_a) + x_3(k_a) \mathbf{R}(t_{k_a}) \mathbf{d}_1(k_a) = \mathbf{s}_1 \\ \vdots \\ \mathbf{x}_1(k_a) + x_{2+L}(k_a) \mathbf{R}(t_{k_a}) \mathbf{d}_L(k_a) = \mathbf{s}_L \end{cases}, \quad (19)$$

and from the output of (3) for $k = k_a$, it must be true that

$$\begin{cases} \mathbf{d}_1(k_a) = \mathbf{R}^T(t_{k_a}) \frac{\mathbf{s}_1 - \mathbf{p}(t_{k_a})}{\|\mathbf{s}_1 - \mathbf{p}(t_{k_a})\|} \\ \vdots \\ \mathbf{d}_L(k_a) = \mathbf{R}^T(t_{k_a}) \frac{\mathbf{s}_L - \mathbf{p}(t_{k_a})}{\|\mathbf{s}_L - \mathbf{p}(t_{k_a})\|} \end{cases}. \quad (20)$$

Rearrange (20) as

$$\begin{cases} \mathbf{p}(t_{k_a}) + \|\mathbf{s}_1 - \mathbf{p}(t_{k_a})\| \mathbf{R}(t_{k_a}) \mathbf{d}_1(k_a) = \mathbf{s}_1 \\ \vdots \\ \mathbf{p}(t_{k_a}) + \|\mathbf{s}_L - \mathbf{p}(t_{k_a})\| \mathbf{R}(t_{k_a}) \mathbf{d}_L(k_a) = \mathbf{s}_L \end{cases}. \quad (21)$$

Under the conditions of the theorem, (10) holds for all α_1 . Taking the differences between the i th and j th equations of both (19) and (21) and comparing the results yields

$$\begin{aligned} & [x_{2+i}(k_a) - \|\mathbf{s}_i - \mathbf{p}(t_{k_a})\|] \mathbf{R}(t_{k_a}) \mathbf{d}_i(k_a) \\ & - [x_{2+j}(k_a) - \|\mathbf{s}_j - \mathbf{p}(t_{k_a})\|] \mathbf{R}(t_{k_a}) \mathbf{d}_j(k_a) = \mathbf{0} \end{aligned}$$

or, equivalently,

$$\begin{aligned} & [x_{2+i}(k_a) - \|\mathbf{s}_i - \mathbf{p}(t_{k_a})\|] \mathbf{d}_i(k_a) \\ & - [x_{2+j}(k_a) - \|\mathbf{s}_j - \mathbf{p}(t_{k_a})\|] \mathbf{d}_j(k_a) = \mathbf{0}. \end{aligned} \quad (22)$$

As (10) holds for all α_1 , it follows from (22) that

$$\begin{cases} x_{2+i}(k_a) = \|\mathbf{s}_i - \mathbf{p}(t_{k_a})\| \\ x_{2+j}(k_a) = \|\mathbf{s}_j - \mathbf{p}(t_{k_a})\| \end{cases}. \quad (23)$$

Now, comparing the i th (or j th) equations of (19) and (21), and using (23), it must be true that

$$\mathbf{x}_1(k_a) = \mathbf{p}(t_{k_a}). \quad (24)$$

Using (24) and comparing (19) with (21) allows us to conclude that

$$\begin{cases} x_3(k_a) = \|\mathbf{s}_1 - \mathbf{p}(t_{k_a})\| \\ \vdots \\ x_{2+L}(k_a) = \|\mathbf{s}_L - \mathbf{p}(t_{k_a})\| \end{cases}. \quad (25)$$

Now compute the output of the linear system (9) for $k = k_a + 1$ as a function of its initial state, giving

$$\begin{aligned} & \mathbf{x}_1(k_a) + T \mathbf{x}_2(k_a) + \mathbf{u}(k_a) \\ & - T \mathbf{d}_i^T(k_a + 1) \mathbf{R}^T(t_{k_a+1}) \mathbf{x}_2(k_a) \mathbf{R}(t_{k_a+1}) \mathbf{d}_i(k_a + 1) \\ & + \mathbf{d}_i^T(k_a + 1) \mathbf{R}^T(t_{k_a+1}) \mathbf{R}(t_{k_a}) \mathbf{d}_i(k_a) x_{2+i}(k_a) \\ & \mathbf{R}(t_{k_a+1}) \mathbf{d}_i(k_a + 1) \\ & - \mathbf{d}_i^T(k_a + 1) \mathbf{R}^T(t_{k_a+1}) \mathbf{u}(k_a) \mathbf{R}(t_{k_a+1}) \mathbf{d}_i(k_a + 1) = \mathbf{s}_i \end{aligned} \quad (26)$$

for all $i \in \{1, \dots, L\}$. To compute the output of the nonlinear system (3) for $k = k_a + 1$ as a function of its initial state, first write

$$\mathbf{d}_i(k_a + 1) = \mathbf{R}^T(t_{k_a+1}) \frac{\mathbf{s}_i - \mathbf{p}(t_{k_a}) - T \mathbf{v}_f(t_{k_a}) - \mathbf{u}(k_a)}{\|\mathbf{s}_i - \mathbf{p}(t_{k_a+1})\|} \quad (27)$$

for all $i \in \{1, \dots, L\}$. Rearrange (27) as

$$\begin{aligned} & \mathbf{p}(t_{k_a}) + T \mathbf{v}_f(t_{k_a}) + \mathbf{u}(k_a) \\ & + \|\mathbf{s}_i - \mathbf{p}(t_{k_a+1})\| \mathbf{R}(t_{k_a+1}) \mathbf{d}_i(k_a + 1) = \mathbf{s}_i \end{aligned} \quad (28)$$

for all $i \in \{1, \dots, L\}$. Following the reasoning used to derive (7), we can express $\|\mathbf{s}_i - \mathbf{p}(t_{k_a+1})\|$ as

$$\begin{aligned} \|\mathbf{s}_i - \mathbf{p}(t_{k_a+1})\| &= -T \mathbf{d}_i^T(k_a + 1) \mathbf{R}^T(t_{k_a+1}) \mathbf{v}_f(t_{k_a}) \\ & + \mathbf{d}_i^T(k_a + 1) \mathbf{R}^T(t_{k_a+1}) \mathbf{R}(t_{k_a}) \mathbf{d}_i(k_a) \|\mathbf{s}_i - \mathbf{p}(t_{k_a})\| \\ & - \mathbf{d}_i^T(k_a + 1) \mathbf{R}^T(t_{k_a+1}) \mathbf{u}(k_a) \end{aligned}$$

for all $i \in \{1, \dots, L\}$. Substituting that in (28) yields

$$\begin{aligned} & \mathbf{p}(t_{k_a}) + T \mathbf{v}_f(t_{k_a}) + \mathbf{u}(k_a) \\ & - T \mathbf{d}_i^T(k_a + 1) \mathbf{R}^T(t_{k_a+1}) \mathbf{v}_f(t_{k_a}) \mathbf{R}(t_{k_a+1}) \mathbf{d}_i(k_a + 1) \\ & + \mathbf{d}_i^T(k_a + 1) \mathbf{R}^T(t_{k_a+1}) \mathbf{R}(t_{k_a}) \mathbf{d}_i(k_a) \\ & \|\mathbf{s}_i - \mathbf{p}(t_{k_a})\| \mathbf{R}(t_{k_a+1}) \mathbf{d}_i(k_a + 1) \\ & - \mathbf{d}_i^T(k_a + 1) \mathbf{R}^T(t_{k_a+1}) \mathbf{u}(k_a) \mathbf{R}(t_{k_a+1}) \mathbf{d}_i(k_a + 1) = \mathbf{s}_i \end{aligned} \quad (29)$$

for all $i \in \{1, \dots, L\}$. Now, comparing (26) with (29) and using (24) and (25) allows us to conclude that

$$\begin{aligned} & T [\mathbf{I} - \mathbf{R}(t_{k_a+1}) \mathbf{d}_i(k_a + 1) \mathbf{d}_i^T(k_a + 1) \mathbf{R}^T(t_{k_a+1})] \\ & [\mathbf{v}_f(t_{k_a}) - \mathbf{x}_2(k_a)] = \mathbf{0} \end{aligned}$$

for all $i \in \{1, \dots, L\}$ or, equivalently,

$$\begin{aligned} & [\mathbf{I} - \mathbf{d}_i(k_a + 1) \mathbf{d}_i^T(k_a + 1)] \mathbf{R}^T(t_{k_a+1}) \\ & [\mathbf{v}_f(t_{k_a}) - \mathbf{x}_2(k_a)] = \mathbf{0} \end{aligned} \quad (30)$$

for all $i \in \{1, \dots, L\}$. Under the conditions of the theorem, (11) holds for all α_2 , which in turn implies that the only solution of (30) is $\mathbf{x}_2(k_a) = \mathbf{v}_f(t_{k_a})$. This concludes the second part of the theorem, as it has been

shown that in the conditions of the theorem, the initial condition of (3) corresponds to that of (9). Notice that, using Theorem 1, the initial condition of (9) is uniquely determined. Additionally, because the two initial conditions match, it follows that the initial condition of (3) is also uniquely determined, thus concluding the proof.

Theorem 2 presents only sufficient observability conditions. In the following theorem these are shown to be necessary if the same interval length is considered.

THEOREM 3 The nonlinear system (3) is observable on $[k_a, k_a + 2]$, in the sense that the initial state $\{\mathbf{p}(t_{k_a}), \mathbf{v}_f(t_{k_a})\}$ is uniquely determined by the input $\{\mathbf{u}(k):k = k_a, k_a + 1\}$ and the output $\{\mathbf{d}_1(k), \dots, \mathbf{d}_L(k):k = k_a, k_a + 1\}$, if and only if the conditions of Theorem 2 hold.

PROOF See Appendix A.

REMARK 1 In short, the observability conditions derived in this paper amount to saying that if there are two consecutive instants such that there are two noncollinear bearing measurements on each instant, then the system is observable. Three important situations should be considered in what concerns the number and configuration of landmarks: 1) If there are at least three noncollinear landmarks, which is a realistic and typical scenario, the system is always observable, as there are always at least two noncollinear bearing measurements; 2) if two landmarks are available, the system is observable if the vehicle stays away from the line formed by the two landmarks; and 3) if there is only one landmark, observability may still be achieved over a longer period—this case falls out of the scope of this paper, and has been treated in [21].

D. Filter Design

The results presented in the previous section are constructive in the sense that the design of an estimator for (3) can be obtained by designing an estimator for the linear discrete-time system (9). This yields estimates, in discrete time, of the position of the vehicle and the velocity of the fluid. As all the required quantities are available to obtain estimates of these quantities in continuous time by open-loop propagation, between discrete-time updates one may use

$$\begin{cases} \hat{\mathbf{p}}(t) = \hat{\mathbf{p}}(t_k) + (t - t_k) \hat{\mathbf{v}}_f(t_k) + \int_{t_k}^t \mathbf{R}(\tau) \mathbf{v}_r(\tau) d\tau \\ \hat{\mathbf{v}}_f(t) = \hat{\mathbf{v}}_f(t_k) \end{cases}, \quad (31)$$

where $t_k < t < t_{k+1}$.

IV. FILTER DESIGN WITHOUT STATE AUGMENTATION

This section presents an alternative method to estimate the position of the vehicle and the velocity of the fluid that does not require state augmentation. In short, a different artificial output, which is linear in the system state, is

obtained, and it is shown that its information suffices to retrieve the state of the system.

In order to construct an artificial output, notice first that as $\mathbf{d}_i, i = 1, \dots, L$, are unit vectors. We have

$$\begin{aligned} \mathbf{d}_i(k) - (\mathbf{d}_i^T(k) \mathbf{d}_i(k)) \mathbf{d}_i(k) \\ = [\mathbf{I} - \mathbf{d}_i(k) \mathbf{d}_i^T(k)] \mathbf{d}_i(k) = \mathbf{0}. \end{aligned} \quad (32)$$

Substituting (1) in (32) allows us to write

$$[\mathbf{I} - \mathbf{d}_i(k) \mathbf{d}_i^T(k)] \mathbf{R}^T(t_k) \frac{\mathbf{s}_i - \mathbf{p}(t_k)}{\|\mathbf{s}_i - \mathbf{p}(t_k)\|} = \mathbf{0},$$

which allows us to express an artificial linear output as

$$\begin{aligned} [\mathbf{I} - \mathbf{d}_i(k) \mathbf{d}_i^T(k)] \mathbf{R}^T(t_k) \mathbf{p}(t_k) \\ = [\mathbf{I} - \mathbf{d}_i(k) \mathbf{d}_i^T(k)] \mathbf{R}^T(t_k) \mathbf{s}_i \end{aligned}$$

for all $i \in \{1, \dots, L\}$.

The solution proposed in this section consists in replacing the nonlinear outputs of (3) with (33), which gives the linear system

$$\begin{cases} \begin{bmatrix} \mathbf{p}(t_{k+1}) \\ \mathbf{v}_f(t_{k+1}) \end{bmatrix} = \mathbf{A}(k) \begin{bmatrix} \mathbf{p}(t_k) \\ \mathbf{v}_f(t_k) \end{bmatrix} + \mathbf{B}\mathbf{u}(k) \\ \mathbf{y}(k) = \mathbf{C}(k) \begin{bmatrix} \mathbf{p}(t_k) \\ \mathbf{v}_f(t_k) \end{bmatrix} \end{cases}, \quad (33)$$

where

$$\mathbf{A}(k) = \begin{bmatrix} \mathbf{I} & T\mathbf{I} \\ \mathbf{0} & \mathbf{I} \end{bmatrix} \in \mathbb{R}^{6 \times 6},$$

$$\mathbf{B} = \begin{bmatrix} \mathbf{I} \\ \mathbf{0} \end{bmatrix} \in \mathbb{R}^{6 \times 3},$$

and

$$\mathbf{C}(k) = \begin{bmatrix} [\mathbf{I} - \mathbf{d}_1(k) \mathbf{d}_1^T(k)] \mathbf{R}^T(t_k) & \mathbf{0} \\ \vdots & \vdots \\ [\mathbf{I} - \mathbf{d}_L(k) \mathbf{d}_L^T(k)] \mathbf{R}^T(t_k) & \mathbf{0} \end{bmatrix} \in \mathbb{R}^{3L \times 6}.$$

The following theorem addresses the observability of (33).

THEOREM 4 The discrete-time linear system (33) is observable on $[k_a, k_a + 2]$ —i.e., the initial state $\{\mathbf{p}(t_{k_a}), \mathbf{v}_f(t_{k_a})\}$ is uniquely determined by the input $\{\mathbf{u}(k):k = k_a, k_a + 1\}$ and the output $\{\mathbf{y}(k):k = k_a, k_a + 1\}$ —if and only if the conditions of Theorem 1 hold.

PROOF See Appendix B.

The filter design follows as in Section III-D, only now an estimator is designed, in discrete time, for the discrete-time linear system (33), whereas the open-loop propagation is given by (31).

V. SIMULATION RESULTS

Numerical simulations are presented and discussed in this section to evaluate the achievable performance with the proposed solutions for navigation based on multiple

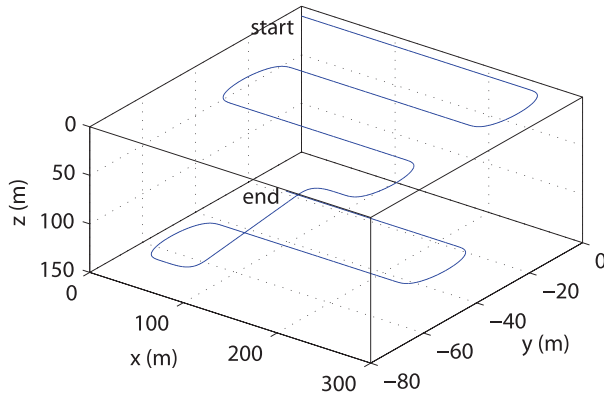


Fig. 1. Trajectory described by vehicle.

bearing measurements. First, the setup that is considered in the simulations is described in Section V-A. In order to evaluate the performance of the proposed solutions, the Bayesian Cramér–Rao bound, briefly described in Section V-B, is computed. The two different proposed solutions are detailed in Sections V-C and V-D. Finally, Monte Carlo results are discussed in Section V-E.

A. Setup

In the simulations, an autonomous underwater vehicle is considered to be moving in the presence of ocean currents. The initial position of the vehicle is set to $\mathbf{p}(0) = [0 \ 0 \ 10]^T$ m, while the ocean-current velocity is set to $\mathbf{v}_c(t) = [0.1 \ -0.2 \ 0]^T$ m/s. The trajectory that is described by the vehicle is shown in Fig. 1. The vehicle is assumed to measure the bearings to a set of three landmarks, whose inertial positions are $\mathbf{s}_1 = [0 \ 0 \ 0]^T$ m, $\mathbf{s}_2 = [500 \ 0 \ 100]^T$ m, and $\mathbf{s}_3 = [0 \ 500 \ 100]^T$ m. Hence, as three noncollinear landmarks are available, the system is observable.

Inclination and azimuth angles to each of the landmarks are assumed to be measured. Hence, the directions are obtained from

$$\mathbf{d}_i = \begin{bmatrix} \sin(\theta_i) \cos(\varphi_i) \\ \sin(\theta_i) \sin(\varphi_i) \\ \cos(\theta_i) \end{bmatrix},$$

$i = 1, 2, 3$, where θ_i and φ_i are, respectively, the inclination and azimuth angles to the i th landmark. A sampling period of $T = 1$ s is considered for these angle measurements, and zero-mean Gaussian noise, with standard deviation of 1° , is also added. The vehicle’s relative velocity, measured by a Doppler velocity log, is assumed to be available at 100 Hz and is corrupted by additive zero-mean Gaussian noise, with standard deviation of 0.01 m/s. The attitude—provided by an AHRS, available at 100 Hz, and parameterized by roll, pitch, and yaw Euler angles—is also assumed to be corrupted by zero-mean additive Gaussian noise, with standard deviation of 0.03° for the roll and pitch and 0.3° for the yaw.

The discrete-time input $\mathbf{u}(k)$, corresponding to a definite integral, is approximated using the trapezoid rule, while the open-loop solution of the position and

ocean-current velocity estimates, between bearing measurements, is computed using the Euler method. In fact, as it also corresponds to a definite integral, it is equivalent to the application of the trapezoid rule.

B. Bayesian Cramér–Rao Bound

Although the optimal design of estimators for nonlinear systems is still an open field of research, there exist some theoretical bounds on achievable performance in some cases. In particular, for a discrete-time system with linear process and nonlinear output, considering additive white Gaussian noise, it is possible to compute the Bayesian Cramér–Rao bound (BCRB), which provides a lower bound on the covariance matrix of any given causal (realizable) unbiased estimator [22].

Consider the general discrete-time system

$$\begin{cases} \mathbf{x}(k+1) = \mathbf{F}(k) \mathbf{x}(k) + \mathbf{B}(k) \mathbf{u}(k) + \mathbf{n}_x(k) \\ \mathbf{y}(k) = \mathbf{h}(\mathbf{x}(k)) + \mathbf{n}_y(k) \end{cases}, \quad (34)$$

where $\mathbf{x}(k)$ is the state vector; $\mathbf{u}(k)$ is a deterministic system input; $\mathbf{y}(k)$ is the system output, which depends on the state vector through the nonlinear function $\mathbf{h}(\mathbf{x}(k))$; $\mathbf{n}_x(k)$ follows a zero-mean Gaussian distribution with covariance $\mathbf{Q}_x(k)$; and $\mathbf{n}_y(k)$ follows a zero-mean Gaussian distribution with covariance $\mathbf{Q}_y(k)$. The recursion that provides the BCRB is similar to that of the EKF, with the difference that the Jacobian of $\mathbf{h}(\mathbf{x}(k+1))$ is evaluated at the true state (see [22, Section 2.3.3]). Using the information matrix representation, the BCRB lower bound $\mathbf{P}_L(k)$ is given by

$$\mathbf{P}_L(k) = \mathbf{J}^{-1}(k),$$

where $\mathbf{J}(k)$ satisfies the recursion

$$\mathbf{J}(k+1) = [\mathbf{Q}_x(k) + \mathbf{F}(k) \mathbf{J}^{-1}(k) \mathbf{F}^T(k)]^{-1} + \mathbf{P}_m(k+1).$$

In this expression, $\mathbf{P}_m(k+1)$ accounts for the covariance reduction due to the observations, given by

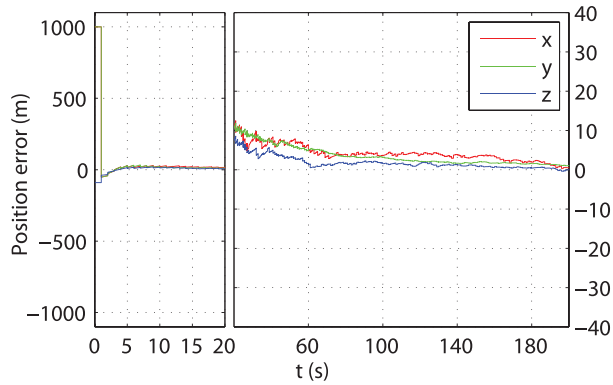
$$\begin{aligned} \mathbf{P}_m(k+1) &= E_{\mathbf{x}(k+1)} \{ \tilde{\mathbf{H}}^T(\mathbf{x}(k+1)) \mathbf{Q}_y^{-1}(k+1) \tilde{\mathbf{H}}(\mathbf{x}(k+1)) \}, \\ & \quad (35) \end{aligned}$$

where $\tilde{\mathbf{H}}(\mathbf{x}(k+1))$ is the Jacobian of the nonlinear observation function evaluated at $\mathbf{x}(k+1)$. The subscript m stands for measurement.

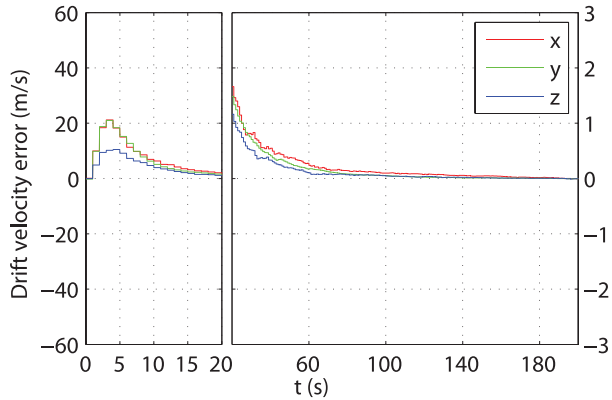
The expectation in (35) is computed with respect to the state vector $\mathbf{x}(k+1)$ and thus is usually evaluated by resorting to Monte Carlo simulations. In nonlinear estimation problems, as in this paper, it is often of interest to evaluate the performance along specific or nominal trajectories $\bar{\mathbf{x}}(k)$. In this case, the term $\mathbf{P}_m(k+1)$ can be simplified to

$$\mathbf{P}_m(k+1) = \tilde{\mathbf{H}}^T(\bar{\mathbf{x}}(k+1)) \mathbf{Q}_y^{-1}(k+1) \tilde{\mathbf{H}}(\bar{\mathbf{x}}(k+1)),$$

which allows assessment of the achievable performance for any tracker or estimator given the specific underlying problem structure. The resulting equations are analogous to the information-filter version of the EKF, whereas the



(a) Position error



(b) Ocean current velocity error

Fig. 2. Initial convergence of errors (filter with state augmentation).

Jacobians are computed at the nominal trajectories $\bar{\mathbf{x}}(k)$ instead of the estimated trajectories, as convincingly argued in [22].

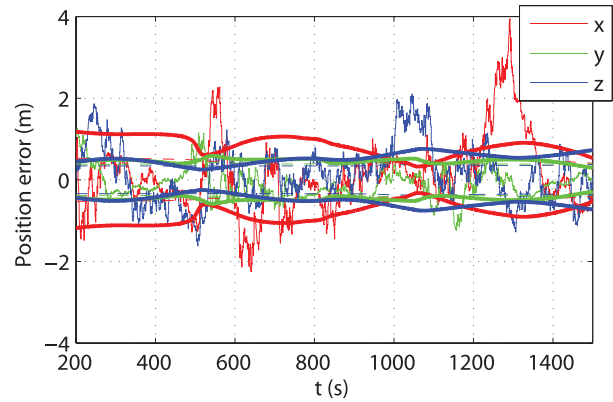
Using inclination and azimuth angles, and considering additive noise in these angles as well as in the relative velocity measurements, the discrete-time system (3) can be written in the form of (34), and hence we can compute the BCRB. This lower bound was computed and is presented in the following.

C. Filter With State Augmentation

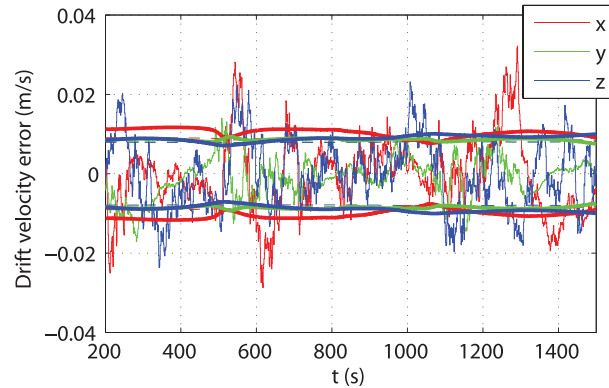
Following the results presented in Section III, a Kalman filter is applied to the augmented system (9), which yields globally exponentially stable error dynamics. To tune the Kalman filter, the state disturbance covariance matrix was chosen as $\text{diag}(0.01^2\mathbf{I}, 0.001^2\mathbf{I}, 10\mathbf{I})$ and the output noise covariance matrix was set to $10\mathbf{I}$. These values were chosen empirically to adjust the performance of the proposed solution with state augmentation.

The initial condition for the position was set at $\hat{\mathbf{x}}_1(0) = [-1000 \ -1000 \ 100]^T$ m, while the ocean-current velocity was set to zero. The states corresponding to the ranges were also set to zero. In this way, the filter was initialized with large position and range errors. The initial covariance of the filter was set to $\text{diag}(10^2\mathbf{I}, \mathbf{I}, \mathbf{I})$.

The initial convergence of the position and velocity errors is depicted in Fig. 2. As can be seen, the error



(a) Position error



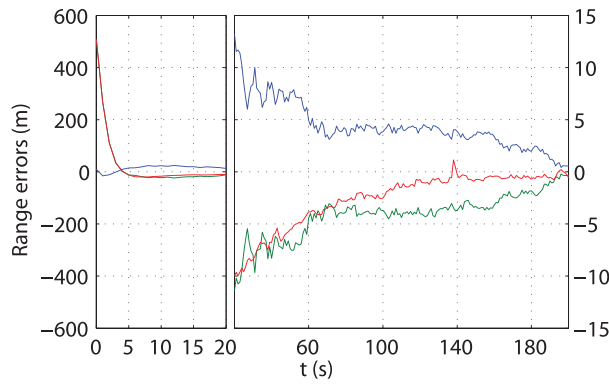
(b) Ocean current velocity error

Fig. 3. Steady-state evolution of errors (filter with state augmentation).

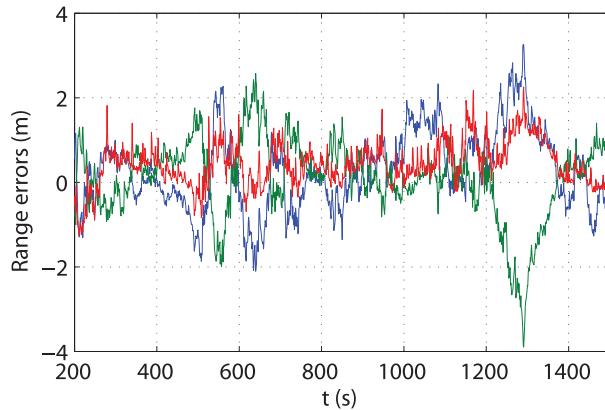
converges very quickly to the neighborhood of 0 (it does not converge to 0 only due to the presence of sensor noise). The detailed evolutions of the position and velocity errors are depicted in Fig. 3. In this plot, the 1σ bounds obtained from the covariance of the Kalman filter (corresponding to the square root of the diagonal elements of the Kalman filter covariance matrix) are depicted in dashed lines. Finally, the 1σ BCRB (more specifically, the square root of the diagonal elements of $\mathbf{P}_L(k)$) is plotted in solid thicker lines. Most noticeable is that the position and velocity errors remain, most of the time, below 2 m and 0.02 m/s, respectively. The achieved performance is consistent with the lower BCRB, and it is also possible to observe that the filter is sometimes slightly overconfident, particularly along the x-coordinate of the position. For the sake of completeness, the evolution of the range errors is shown in Fig. 4.

D. Filter Without State Augmentation

In this section, a Kalman filter is applied to the alternative system proposed in Section IV. To tune the Kalman filter, the state disturbance covariance matrix was chosen as $\text{diag}(0.01^2\mathbf{I}, 0.001^2\mathbf{I})$ and the output noise covariance matrix was set to $10\mathbf{I}$. These values were chosen empirically to adjust the performance of the proposed solution without state augmentation. All initial



(a) Initial convergence



(b) Steady-state evolution

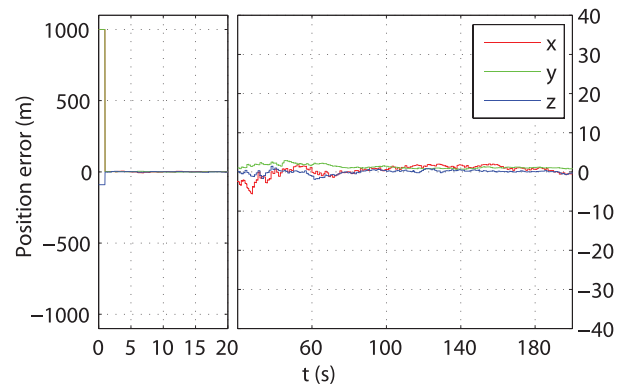
Fig. 4. Evolution of range errors (filter with state augmentation).

conditions were set as before, only now there are no additional states corresponding to the ranges.

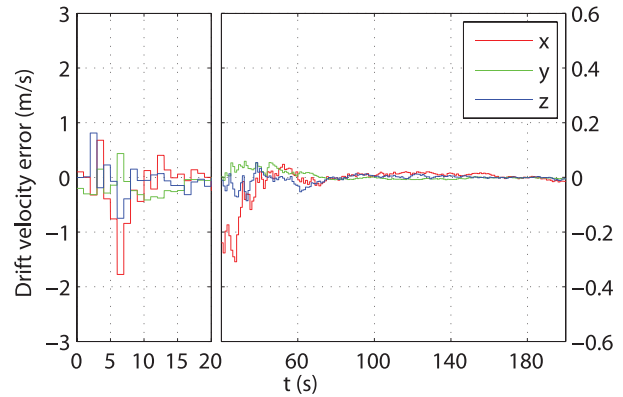
The initial convergence of the position and velocity errors is depicted in Fig. 5. As can be seen, the error converges very quickly to the neighborhood of 0 (it does not converge to 0 only due to the presence of sensor noise). Comparing Figs. 2 and 5, one can conclude that the filter with state augmentation converges slightly slower than the one without state augmentation, which perhaps can be explained by the additional burden of also estimating the distances. The detailed evolutions of the position and velocity errors are depicted in Fig. 6, along with the 1σ bounds obtained from the Kalman-filter covariance matrix and the BCRB, just as in Fig. 3. The most noticeable feature is, again, that the position and velocity errors remain most of the time below 2 m and 0.02 m/s, respectively. The steady-state performance is very similar to that obtained with the filter with state augmentation.

E. Performance Comparison

The proposed solutions were compared with the EKF applied to the original nonlinear system (3). The initial estimates were set as in the previous simulation. In order to achieve good performance, the state disturbance matrix was set to $\text{diag}(0.01^2\mathbf{I}, 0.001^2\mathbf{I})$ and the output noise covariance matrix was set to $(2 \times 10^{-5})\mathbf{I}$.



(a) Position error

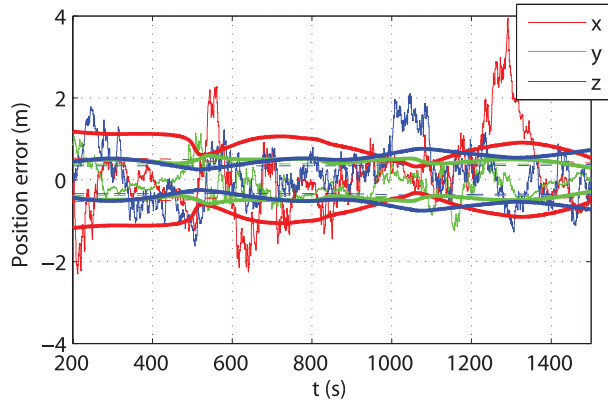


(b) Ocean current velocity error

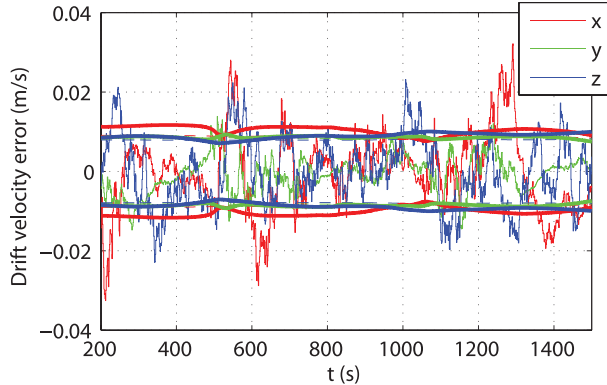
Fig. 5. Initial convergence of errors (filter without state augmentation).

The initial convergence of the position and velocity errors is depicted in Fig. 7. In comparison with the proposed solutions, the EKF exhibits a slightly slower convergence and much larger initial transients. The detailed evolutions of the position and velocity errors are depicted in Fig. 8, along with the 1σ bounds obtained from the EKF covariance matrix and the BCRB. The EKF performs, in steady state, similarly to the proposed solutions. It does not, however, offer global convergence guarantees.

Finally, in order to better evaluate the performance of the proposed solutions, the Monte Carlo method was applied, and 1000 simulations were carried out with different, randomly generated noise signals. The standard deviation of the errors were computed in steady state (for $t \geq 360$ s) for each simulation and averaged over the set of simulations. The results are depicted in Table I. The results with the EKF are also included. Additionally, the average steady-state 1σ BCRB was computed (for $t \geq 360$ s), as shown in Table I. Comparing the performance of the proposed solutions, as well as that of the EKF, it can be seen that they are all very similar. Notice that the proposed solutions may achieve smaller standard deviation than the theoretical BCRB. This is so because the BCRB assumes an unbiased estimator, whereas the proposed solutions may be slightly biased, which is not uncommon in nonlinear estimation problems.



(a) Position error



(b) Ocean current velocity error

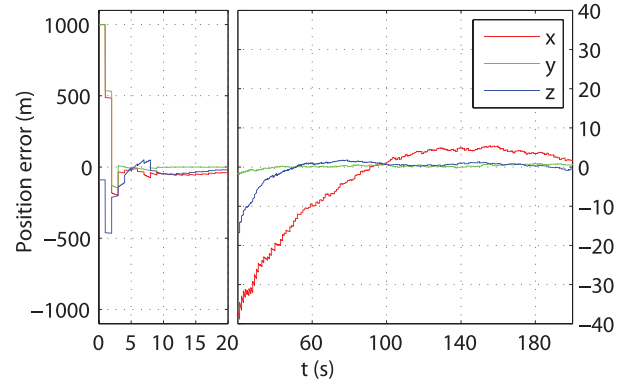
Fig. 6. Steady-state evolution of errors (filter without state augmentation).

TABLE I
Standard Deviation of the Steady-State Estimation Error, Averaged Over 1000 Runs of the Simulation

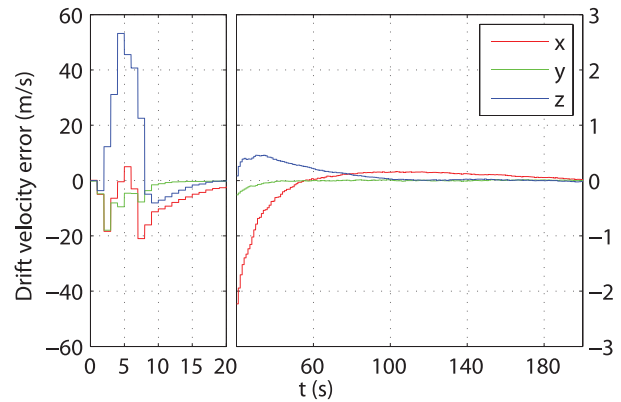
Variable (Unit)	With State Augmentation	Without State Augmentation
$\hat{\mathbf{p}}_x$ (m)	89.4×10^{-2}	89.4×10^{-2}
$\hat{\mathbf{p}}_y$ (m)	41.5×10^{-2}	41.4×10^{-2}
$\hat{\mathbf{p}}_z$ (m)	70.0×10^{-2}	70.7×10^{-2}
$\tilde{\mathbf{v}}_{fx}$ (m/s)	9.72×10^{-3}	9.72×10^{-3}
$\tilde{\mathbf{v}}_{fy}$ (m/s)	4.96×10^{-3}	5.00×10^{-3}
$\tilde{\mathbf{v}}_{fz}$ (m/s)	9.06×10^{-3}	9.06×10^{-3}
Variable (Unit)	EKF	Average BCRB
$\hat{\mathbf{p}}_x$ (m)	88.4×10^{-2}	79.6×10^{-2}
$\hat{\mathbf{p}}_y$ (m)	44.4×10^{-2}	46.2×10^{-2}
$\hat{\mathbf{p}}_z$ (m)	65.0×10^{-2}	52.6×10^{-2}
$\tilde{\mathbf{v}}_{fx}$ (m/s)	12.2×10^{-3}	10.2×10^{-3}
$\tilde{\mathbf{v}}_{fy}$ (m/s)	8.37×10^{-3}	8.57×10^{-3}
$\tilde{\mathbf{v}}_{fz}$ (m/s)	11.9×10^{-3}	8.92×10^{-3}

VI. CONCLUSIONS

This paper addressed the problem of navigation based on multiple bearing measurements, and two different solutions were proposed. First, the observability of the system was addressed and sufficient and necessary conditions were derived. The observability analyses were constructive, and in both cases, the discrete-time nature of the bearing measurements was taken into account and



(a) Position error



(b) Ocean current velocity error

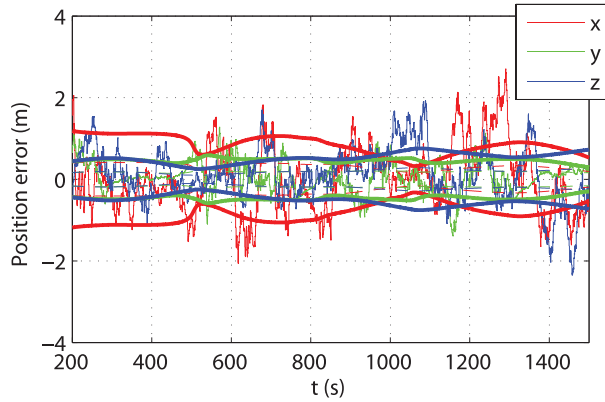
Fig. 7. Initial convergence of EKF errors.

globally exponentially stable error dynamics achieved with the design of estimators for linear systems. This is a result of appropriate state augmentation and output transformations that allow consideration of linear systems for a problem that is originally nonlinear, without resorting to any kind of approximations. Simulation results were discussed, including a comparison with the extended Kalman filter and the Bayesian Cramér–Rao bound, as well as Monte Carlo runs. In short, the proposed filters achieve performances that are tight to the theoretical lower bound and at the same time provide global convergence guarantees. In terms of computational complexity, the solution with state augmentation has more states than both the solution without state augmentation and the EKF, which have the same number of states.

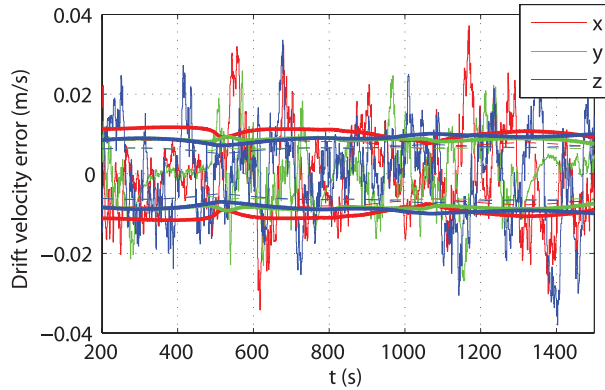
APPENDIX A PROOF OF THEOREM 3

The sufficiency part of Theorem 3 is shown in Theorem 2, and thus only the necessity of the conditions needs to be established. Suppose first that (10) does not hold. That means that all directions are identical for $k = k_a$. Let $\mathbf{d}_i^u(k)$, $k = k_a, k_a + 1$, denote the output of the nonlinear system (3) with initial condition

$$\begin{cases} \mathbf{p}^u(t_{k_a}) = \mathbf{p}^o \\ \mathbf{v}_f^u(t_{k_a}) = \mathbf{v}_f^o \end{cases}$$



(a) Position error



(b) Ocean current velocity error

Fig. 8. Steady-state evolution of EKF errors.

and input $\mathbf{u}(k)$, $k = k_a, k_a + 1$ —i.e.,

$$\begin{cases} \mathbf{d}_i^u(k_a) = \frac{\mathbf{s}_i - \mathbf{p}^o}{\|\mathbf{s}_i - \mathbf{p}^o\|} =: \mathbf{d}^o \\ \mathbf{d}_i^u(k_a + 1) = \frac{\mathbf{s}_i - \mathbf{p}^o - T\mathbf{v}_s^o - \mathbf{u}(k_a)}{\|\mathbf{s}_i - \mathbf{p}^o - T\mathbf{v}_s^o - \mathbf{u}(k_a)\|} \end{cases}$$

for all $i \in \{1, \dots, L\}$. Consider a different initial condition

$$\begin{cases} \mathbf{p}^v(t_{k_a}) = \mathbf{p}^o - \alpha \mathbf{d}^o \\ \mathbf{v}_f^v(t_{k_a}) = \mathbf{v}_s^o + \frac{\alpha}{T} \mathbf{d}^o \end{cases}$$

with $\alpha > 0$, and denote by $\mathbf{d}_i^v(k)$, $k = k_a, k_a + 1$, the corresponding output for the same input. Then

$$\begin{aligned} \mathbf{d}_i^v(k_a) &= \frac{\mathbf{s}_i - \mathbf{p}^o + \alpha \mathbf{d}^o}{\|\mathbf{s}_i - \mathbf{p}^o + \alpha \mathbf{d}^o\|} = \frac{(\|\mathbf{s}_i - \mathbf{p}^o\| + \alpha) \mathbf{d}^o}{\|(\|\mathbf{s}_i - \mathbf{p}^o\| + \alpha) \mathbf{d}^o\|} \\ &= \mathbf{d}^o = \mathbf{d}_i^u(k_a) \end{aligned}$$

and

$$\begin{aligned} \mathbf{d}_i^v(k_a + 1) &= \frac{\mathbf{s}_i - \mathbf{p}^o + \alpha \mathbf{d}^o - T\mathbf{v}_s^o - \alpha \mathbf{d}^o - \mathbf{u}(k_a)}{\|\mathbf{s}_i - \mathbf{p}^o + \alpha \mathbf{d}^o - T\mathbf{v}_s^o - \alpha \mathbf{d}^o - \mathbf{u}(k_a)\|} \\ &= \frac{\mathbf{s}_i - \mathbf{p}^o - T\mathbf{v}_s^o - \mathbf{u}(k_a)}{\|\mathbf{s}_i - \mathbf{p}^o - T\mathbf{v}_s^o - \mathbf{u}(k_a)\|} = \mathbf{d}_i^u(k_a + 1) \end{aligned}$$

for all $i \in \{1, \dots, L\}$. It has been shown that if (10) does not hold, then there exist at least two initial conditions such that the system output is identical, which means that the nonlinear system (3) is not observable.

Suppose now that (11) does not hold. That means that all directions are identical for $k = k_a + 1$. Let $\mathbf{d}_i^u(k)$, $k = k_a, k_a + 1$, denote the output of the nonlinear system (3) with initial condition

$$\begin{cases} \mathbf{p}^u(t_{k_a}) = \mathbf{p}^o \\ \mathbf{v}_f^u(t_{k_a}) = \mathbf{v}_s^o \end{cases}$$

and input $\mathbf{u}(k)$, $k = k_a, k_a + 1$ —i.e.,

$$\begin{cases} \mathbf{d}_i^u(k_a) = \frac{\mathbf{s}_i - \mathbf{p}^o}{\|\mathbf{s}_i - \mathbf{p}^o\|} \\ \mathbf{d}_i^u(k_a + 1) = \frac{\mathbf{s}_i - \mathbf{p}^o - T\mathbf{v}_s^o - \mathbf{u}(k_a)}{\|\mathbf{s}_i - \mathbf{p}^o - T\mathbf{v}_s^o - \mathbf{u}(k_a)\|} =: \mathbf{d}^o \end{cases}$$

for all $i \in \{1, \dots, L\}$. Consider a different initial condition

$$\begin{cases} \mathbf{p}^v(t_{k_a}) = \mathbf{p}^o \\ \mathbf{v}_f^v(t_{k_a}) = \mathbf{v}_s^o - \frac{\alpha}{T} \mathbf{d}^o \end{cases}$$

with $\alpha > 0$, and denote by $\mathbf{d}_i^v(k)$, $k = k_a, k_a + 1$, the corresponding output for the same input. Then

$$\mathbf{d}_i^v(k_a) = \frac{\mathbf{s}_i - \mathbf{p}^o}{\|\mathbf{s}_i - \mathbf{p}^o\|} = \mathbf{d}_i^u(k_a)$$

and

$$\begin{aligned} \mathbf{d}_i^v(k_a + 1) &= \frac{\mathbf{s}_i - \mathbf{p}^o - T\mathbf{v}_s^o + \alpha \mathbf{d}^o - \mathbf{u}(k_a)}{\|\mathbf{s}_i - \mathbf{p}^o - T\mathbf{v}_s^o + \alpha \mathbf{d}^o - \mathbf{u}(k_a)\|} \\ &= \frac{(\|\mathbf{s}_i - \mathbf{p}^o - T\mathbf{v}_s^o - \mathbf{u}(k_a)\| + \alpha) \mathbf{d}^o}{\|(\|\mathbf{s}_i - \mathbf{p}^o - T\mathbf{v}_s^o - \mathbf{u}(k_a)\| + \alpha) \mathbf{d}^o\|} \\ &= \mathbf{d}^o = \mathbf{d}_i^u(k_a + 1) \end{aligned}$$

for all $i \in \{1, \dots, L\}$. It has been shown that if (11) does not hold, then there exist at least two initial conditions such that the system output is identical, which means that the nonlinear system (3) is not observable. This concludes the proof, as it has been shown that if either (10) or (11) does not hold, then the system is not observable, and thus both conditions are necessary for the nonlinear system (3) to be observable.

APPENDIX B PROOF OF THEOREM 4

The proof amounts to showing that the observability matrix $\mathbf{O}(k_a, k_a + 2)$ associated with the pair $(\mathbf{A}(k), \mathbf{C}(k))$ on $[k_a, k_a + 2]$ has rank equal to the number of states of the system if and only if both (10) and (11) hold for some $i, j, l, m \in \{1, \dots, L\}$. Suppose that the system is not observable and both (10) and (11) hold for some $i, j, l, m \in \{1, \dots, L\}$. Then there exists a unit vector

$$\mathbf{c} = \begin{bmatrix} \mathbf{c}_1 \\ \mathbf{c}_2 \end{bmatrix} \in \mathbb{R}^6,$$

$$\mathbf{c}_1, \mathbf{c}_2 \in \mathbb{R}^3,$$

such that $\mathbf{O}(k_a, k_a + 2)\mathbf{c} = \mathbf{0}$ or, equivalently,

$$\begin{cases} \mathbf{C}(k_a)\mathbf{c} = \mathbf{0} \\ \mathbf{C}(k_a + 1)\mathbf{A}(k_a)\mathbf{c} = \mathbf{0} \end{cases} \quad (36)$$

From the first equation of (36) we have

$$\begin{cases} [\mathbf{I} - \mathbf{d}_1(k_a) \mathbf{d}_1^T(k_a)] \mathbf{R}^T(t_{k_a}) \mathbf{c}_1 = \mathbf{0} \\ \vdots \\ [\mathbf{I} - \mathbf{d}_L(k_a) \mathbf{d}_L^T(k_a)] \mathbf{R}^T(t_{k_a}) \mathbf{c}_1 = \mathbf{0} \end{cases} \quad (37)$$

If (10) holds for some $i, j \in \{1, \dots, L\}$, then the only solution of (37) is $\mathbf{c}_1 = \mathbf{0}$. Substituting that in the second equation of (36) gives

$$\begin{cases} T [\mathbf{I} - \mathbf{d}_1(k_a + 1) \mathbf{d}_1^T(k_a + 1)] \mathbf{R}^T(t_{k_a+1}) \mathbf{c}_2 = \mathbf{0} \\ \vdots \\ T [\mathbf{I} - \mathbf{d}_L(k_a + 1) \mathbf{d}_L^T(k_a + 1)] \mathbf{R}^T(t_{k_a+1}) \mathbf{c}_2 = \mathbf{0} \end{cases} \quad (38)$$

As (11) is assumed to hold for some $l, m \in \{1, \dots, L\}$, the only solution of (38) is $\mathbf{c}_2 = \mathbf{0}$. But this contradicts the hypothesis of the existence of a unit vector \mathbf{c} such that (36) holds. If both (10) and (11) hold for some $i, j, l, m \in \{1, \dots, L\}$, then the system is observable, thus concluding the proof of sufficiency.

To show necessity, suppose first that (10) is not verified. Then, for $k = k_a$, all directions are identical. Let $\mathbf{d}_i(k_a) = \mathbf{d}^o$ for all $i = 1, \dots, L$ and let

$$\mathbf{c} = \begin{bmatrix} \mathbf{R}(t_{k_a}) \mathbf{d}^o \\ \mathbf{0} \end{bmatrix}.$$

Then $\mathbf{O}(k_a, k_a + 2)\mathbf{c} = \mathbf{0}$, which means that the system is not observable. Suppose now that (11) is not verified. Then, for $k = k_a + 1$, all directions are identical. Let $\mathbf{d}_i(k_a + 1) = \mathbf{d}^o$ for all $i = 1, \dots, L$ and let

$$\mathbf{c} = \begin{bmatrix} \mathbf{0} \\ \mathbf{R}(t_{k_a+1}) \mathbf{d}^o \end{bmatrix}.$$

Then $\mathbf{O}(k_a, k_a + 2)\mathbf{c} = \mathbf{0}$, which means that the system is not observable. Therefore, if either (10) or (11) is not verified, the system (33) is not observable, which implies that if (33) is observable, then both (10) and (11) must hold, therefore concluding the proof of necessity.

REFERENCES

- [1] Sukkariéh, S., Nebot, E. M., and Durrant-Whyte, H. F. A high integrity IMU/GPS navigation loop for autonomous land vehicle applications. *IEEE Transactions on Robotics and Automation*, **15**, 3 (June 1999), 572–578.
- [2] Techy, L., Morgansen, K. A., and Woolsey, C. A. Long-baseline acoustic localization of the Seaglider underwater glider. In *2011 American Control Conference*, San Francisco, CA, June–July 2011, 3990–3995.
- [3] Whitcomb, L. L., Yoerger, D. R., and Singh, H. Combined Doppler/LBL based navigation of underwater vehicles. In *11th International Symposium on Unmanned Untethered Submersible Technology*, Durham, NH, Aug. 1999.
- [4] Vaganay, J., Bellingham, J. G., and Leonard, J. J. Comparison of fix computation and filtering for autonomous acoustic navigation. *International Journal of Systems Science*, **29**, 10 (1998), 1111–1122.
- [5] Kinsey, J. C., and Whitcomb, L. L. Preliminary field experience with the DVLNAV integrated navigation system for manned and unmanned submersibles. In *Proceedings of the 1st IFAC Workshop on Guidance and Control of Underwater Vehicles*, Newport, UK, Apr. 2003, 83–88.
- [6] Jouffroy, J., and Opderbecke, J. Underwater vehicle trajectory estimation using contracting PDE-based observers. In *Proceedings of the 2004 American Control Conference*, Boston, MA, June–July 2004, **5**, 4108–4113.
- [7] Indiveri, G., Pedone, P., and Cuccovillo, M. Fixed target 3D localization based on range data only: A recursive least squares approach. In *Proceedings of the 3rd IFAC Conference on Navigation, Guidance, and Control of Underwater Vehicles*, Porto, Portugal, April 2012.
- [8] Gadre, A. S., and Stilwell, D. J. A complete solution to underwater navigation in the presence of unknown currents based on range measurements from a single location. In *2005 IEEE/RSJ International Conference on Intelligent Robots and Systems*, Edmonton, Canada, Aug. 2005, 1420–1425.
- [9] Jouffroy, J., and Reger, J. An algebraic perspective to single-transponder underwater navigation. In *2006 IEEE International Conference on Control Applications*, Munich, Germany, Oct. 2006, 1789–1794.
- [10] Lee, P.-M., Jun, B.-H., Kim, K., Lee, J., Aoki, T., and Hyakudome, T. Simulation of an inertial acoustic navigation system with range aiding for an autonomous underwater vehicle. *IEEE Journal of Oceanic Engineering*, **32**, 2 (Apr. 2007), 327–345.
- [11] Batista, P., Silvestre, C., and Oliveira, P. Single range aided navigation and source localization: Observability and filter design. *Systems & Control Letters*, **60**, 8 (Aug. 2011), 665–673.
- [12] Deghat, M., Shames, I., Anderson, B. D. O., and Yu, C. Target localization and circumnavigation using bearing measurements in 2D. In *49th IEEE Conference on Decision and Control*, Atlanta, GA, Dec. 2010, 334–339.
- [13] Nardone, S. C., and Aidala, V. J. Observability criteria for bearings-only target motion analysis. *IEEE Transactions on Aerospace and Electronic Systems*, **AES-17**, 2 (Mar. 1981), 162–166.
- [14] Hammel, S. E., and Aidala, V. J. Observability requirements for three-dimensional tracking via angle measurements. *IEEE Transactions on Aerospace and Electronic Systems*, **AES-21**, 2 (Mar. 1985), 200–207.
- [15] Briechle, K., and Hanebeck, U. D. Localization of a mobile robot using relative bearing measurements. *IEEE Transactions on Robotics and Automation*, **20**, 1 (Feb. 2004), 36–44.
- [16] Le Cadre, J.-P., and Jauffret, C. Discrete-time observability and estimability analysis for bearings-only target motion analysis. *IEEE Transactions on Aerospace and Electronic Systems*, **33**, 1 (Jan. 1997), 178–201.
- [17] Bréhard, T., and Le Cadre, J.-P. Closed-form posterior Cramér–Rao bounds for bearings-only tracking.

- IEEE Transactions on Aerospace and Electronic Systems*, **42**, 4 (Oct. 2006), 1198–1223.
- [18] Bréhard, T., and Le Cadre, J.-P. Hierarchical particle filter for bearings-only tracking. *IEEE Transactions on Aerospace and Electronic Systems*, **43**, 4 (Oct. 2007), 1567–1585.
- [19] Leong, P. H., Arulampalam, S., Lamahewa, T. A., and Abhayapala, T. D. A Gaussian-sum based cubature Kalman filter for bearings-only tracking. *IEEE Transactions on Aerospace and Electronic Systems*, **49**, 2 (Apr. 2013), 1161–1176.
- [20] Batista, P., Silvestre, C., and Oliveira, P. Globally exponentially stable filters for source localization and navigation aided by direction measurements. *Systems & Control Letters*, **62**, 11 (Nov. 2013), 1065–1072.
- [21] Batista, P., Silvestre, C., and Oliveira, P. GES source localization and navigation based on discrete-time bearing measurements. In *IEEE 52nd Annual Conference on Decision and Control*, Florence, Italy, Dec. 2013, 5066–5071.
- [22] Van Trees, H. L., and Bell, K. L. (Eds.) *Bayesian Bounds for Parameter Estimation and Nonlinear Filtering/Tracking*. Piscataway, NJ: Wiley, 2007.



Pedro Batista (M'10) received a Licenciatura degree in electrical and computer engineering in 2005 and a Ph.D. degree in 2010, both from Instituto Superior Técnico (IST), Lisbon, Portugal. From 2004 to 2006, he was a monitor with the department of mathematics, IST, where he is currently an invited assistant professor in the department of electrical and computer engineering. His research interests include sensor-based navigation and control of autonomous vehicles. Dr. Batista has received the Diploma de Mérito twice, and his Ph.D. degree thesis was awarded the Best Robotics Ph.D. Thesis Award by the Portuguese Society of Robotics.



Carlos Silvestre (M'07) received a Licenciatura degree in electrical engineering from the Instituto Superior Técnico (IST) of Lisbon, Portugal, in 1987, and an M.Sc. degree in electrical engineering and a Ph.D. degree in control science from the same school in 1991 and 2000, respectively. In 2011 he received a habilitation in electrical engineering and computers, also from IST. Since 2000 he has been with the department of electrical engineering of IST, where he is currently an associate professor of control and robotics on leave. As of 2015 he is a professor of the department of electrical and computers engineering in the Faculty of Science and Technology of the University of Macau. Over the past years, he has conducted research on the subjects of navigation guidance and control of air and underwater robots. His research interests include linear and nonlinear control theory, coordinated control of multiple vehicles, gain-scheduled control, integrated design of guidance and control systems, inertial navigation systems, and mission control and real-time architectures for complex autonomous systems with applications to unmanned air and underwater vehicles.



Paulo Oliveira (SM'10) received a Ph.D. degree in 2002 from the Instituto Superior Técnico (IST), Lisbon, Portugal. He is currently an associate professor with the department of mechanical engineering at IST, as well as a researcher in the IDMEC/LAETA and collaborator in the ISR/LARSyS, Lisbon, Portugal. His research interests include mechatronics, robotics, and estimation, with special focus on the fields of sensor fusion, navigation, and control. He has participated in more than 20 Portuguese and European research projects over the last 25 years.